Turk J Phys
28 (2004) , 325 – 340.

Polar Optical Phonon Modes and Fröhlich Electron-Phonon Interaction Hamiltonians in Coaxial Cylindrical Quantum Cables

Li ZHANG, Hong Jing XIE
Department of Mechanics and Electronics, Panyu Polytechnic, Panyu, 511483, P.R. CHINA
e-mail: zhangli-gz@263.net

Received 31.10.2003

Abstract

By using the dielectric continuum approximation, the polar optical phonon modes of coaxial cylindrical quantum cables with arbitrary layer-number were studied. In order to describe the vibrating of the longitudinal-optical (LO) phonons, a set of legitimate eigenfunctions for LO phonon modes are constructed and adopted. In order to deal with the interface optical (IO) phonon modes, the transfer matrix method is employed. The quantized LO and IO phonons fields, as well as their corresponding Fröhlich electron-phonon interaction Hamiltonians, are also derived. Numerical calculations on a four-layer GaAs/$Al_xGa_{1-x}As$ QC have been performed. Results reveal that there are six branches of IO phonon modes. When the wave vector k_z in the z direction and the azimuthal quantum number m are small, the dispersion frequencies of IO modes sensitively depend on k_z and m, and the frequency forbidden behaviors of IO phonon modes were observed and the reason was analyzed. When k_z and m are relatively large, with increasing k_z and m, the frequency for each mode converges to the limit frequency value of IO mode in a single heterostructure, and the electrostatic potential distribution of each branch of IO mode tends to be more and more localized at some interface; meanwhile, the coupling between the electron-IO phonon becomes weaker and weaker. The calculation also shows that the phonon modes with higher frequencies have more significant contribution to the electron-phonon interaction. At last, it is found that k_z and m have analogous influences on the frequencies and the electrostatic potentials of the IO phonons.

Key Words: Optical Phonon Modes; Coaxial Cylindrical Quantum Cables.
PACS: 63.20.Dj; 73.61.Ga; 63.20.Kr; 73.21.Ac

1. Introduction

During the last decade, with the rapid progress in semiconductor nanotechnology, such as molecular-beam epitaxy, metal-organic chemical-vapor deposition and chemical lithography, not only multi-layer planar quantum wells (QWs), but also many sophisticated curve-surface semiconductor heterostructures are now able to be fabricated. For example, in 1993, by using the method of wet chemical synthesis, Eychmüller et al. [1] synthesized the inhomogeneous spherical quantum dot (QD) with an centric core barrier and several shell wells, which were called quantum dot quantum well (QDQW). The experimental [2, 3] and theoretical works [4–7] on QDQWs reveal that, due to their inner configurations for electrons and holes,

many physical properties in these systems are obviously different from those in homogeneous QDs. In 1997 and 1998, by means of reactive laser ablation, Suenaga and Zhang' group [8, 9] successfully synthesized the inhomogeneous coaxial cylindrical quantum-well wires (QWW), termed quantum cables (QC). On the basis of these structures brought forward, Zeng et al. [10] predicted the single-electron subband properties in a five-layer GaAlAs/GaAs inhomogeneous QWW systems, and the systems exhibit some interesting and unique behaviors unexpected in other nanostructures. Recently, Aktas et al. [11] studied the ground state binding energy of a impurity in a four-layer coaxial QWW system with an applied electric field. Meanwhile, in these low-dimensional quantum systems, it is well-known that the phonons are also confined, which makes the phonon modes more complicated than those in bulk materials [12]. Furthermore, the electron-phonon interaction in these confined systems is one of the important aspects in determining their properties in physical processes, such as in the transport process or the electron relaxation process. Therefore, in order to describe the coupling between electron and phonon properly in the low-dimensional quantum systems, a trustworthy phonon mode and electron-phonon interaction Hamiltonian are essential.

Since the pioneer works of Licari [13] and Fuchs [14] on the phonon modes in confined quantum systems, several authors have made their contributions in studying the phonon modes and electron-phonon interaction in various low-dimensional quantum systems by adopting various theoretical models such as the dielectric continuum (DC) model [15–20, 23, 28–37], the Hydrodynamic model [21, 22], Huang-Zhu (HZ) models [23] and the microscopic calculation model [24–27]. Among them, the DC model had been widely used for its simplicity and efficiency. Wendler and Haupt [15] developed the framework of the theory of optical phonons and electron-phonon interaction for the spatially confined systems. Mori and Ando [16] have investigated the phonon modes in single and double heterostructures QW within the framework of DC approach. Liang and Wang [17] have derived the transverse-optical (TO) and longitudinal-optical (LO) modes as well as four branches of interface optical modes in a GaSb-InAs-GaSb QW. Jun-jie Shi et al. [18] have studied the phonon modes in the coupled and step QWs with four and five layers of GaAs/$Al_xGa_{1-x}As$, and the electron-phonon interaction Fröhlich Hamiltonian were also given and the electron-interface phonon coupling functions were discussed. By using transfer matrix method, Yan et al. [19] and Yu et al. [20] deduced and discussed the interface optical-phonon modes in asymmetric double-barrier structures and in multiple-interface plane heterostructure systems, respectively.

The optical phonon modes in homogeneous QWWs have also been sufficiently investigated. For rectangular QWWs, microscopic calculations of the phonon dispersion have been reported in Refs. [24–26], and macroscopic DC approximations have been adopted to deduce the confined LO and surface optical (SO) phonon modes in Refs. [28, 29]. For cylindrical QWWs, Comas et al. [30] studied the optical phonon modes and electron-phonon interaction Hamiltonian in quantum wire and free-standing quantum wire based on a Lagrangian formalism and phenomenological treatment, respectively; Bergues and co-workers [31] presented a complete description of the phonon modes in the cylindrical QWW systems, including a correct treatment of the mechanical and electrostatic matching conditions at the surface; Wang and Lei [32] described the LO and SO phonons as well as the corresponding Fröhlich couplings with electrons by using DC model, hydrodynamic continuum model and HZ models [23]; Constantinou and Ridley [21] and Enderlein [22] also used the Hydrodynamic continuum model to study the optical modes in wires of circular geometry; Recently, Xie et al. [33] have studied the phonon modes and derived the electron-phonon interaction Hamiltonians in cylindrical QWWs with infinite and finite potential boundary conditions. For QWWs of arbitrary cross-section shapes (including the elliptical QWWs), Bennett et al. [34] and Knipp et al. [35] have also investigated the LO and interface optical (IO) phonons under DC models. Klimin et al. [36] have determined the vibrational modes of inertial polarization in the multilayer QWW and QD, and they calculated the polaron ground state energy as well as the effective mass in the cylindrical QWW and polaronic shift of electron energy levels in the spherical QD. More recently, we investigated the phonon modes and electron- phonon interaction Hamiltonians in multilayer spherical inhomogeneous QD systems under the DC approximation [37]. However, to our knowledge, the optical phonon modes and their interactions with electron in some

inhomogeneous QWWs, such as in multilayer coaxial cylindrical QCs, have not been investigated in detail. Thus, in the current work, a multilayer coaxial QC model is chosen, and the DC approximation is adopted.

The main extents of this work are that, (i) the works of optical phonon mode have been extended from multi-layer QW systems [18–20] and multi-layer inhomogeneous QD systems [37] to inhomogeneous QC system; (ii) In order to describe the vibrating of the LO phonons, a set of legitimate eigenfunctions for LO phonon modes are constructed. In order to treat the interface optical (IO) phonon modes, the transfer matrix method [19, 20] has been employed to deal with the dispersion relation and the coefficients in functions of phonon electrostatic potential in multilayer coaxial cylindrical QCs; (iii) the orthonormal relations for the polarization vector of all the phonon modes in the QC have been obtained, and via the orthonormal relations and the dynamic equation of motion of the crystal lattice, the Fröhlich electron-phonon interaction Hamiltonians have been derived; (iv) when the wave-vectors k_z in z direction and azimuthal quantum number m approach 0 and infinity, respectively, the limit frequencies of IO phonons have been analyzed. It is found that, as k_z and $m \to 0$, the frequency forbidden behaviors of IO phonons in the QC have been observed, which is obviously different from the case in multilayer asymmetrical planar QWs [18]. When k_z or $m \to \infty$, the IO phonons frequencies converge to those in corresponding single heterostructures; (v) the IO phonon potential distributions, and the electron-IO phonon coupling functions have been analyzed and specified, and the detailed comparison for these characters between the inhomogeneous QD and inhomogeneous QC systems has been exhibited. The model of the multilayer coaxial QC is given in Figure 1.

The paper is organized as follows. The confined LO phonon modes and IO phonon modes as well as the corresponding Fröhlich electron-phonon interaction Hamiltonians are deduced in section 2. As an example, the numerical results for the dispersion relation, the electron-phonon coupling functions of the IO phonon modes for a four layers $Ga_{1-x}Al_xAs/GaAs$ QC system are carried out and discussed in section 3. In section 4, we summarized the main results and gave some extended conclusions.

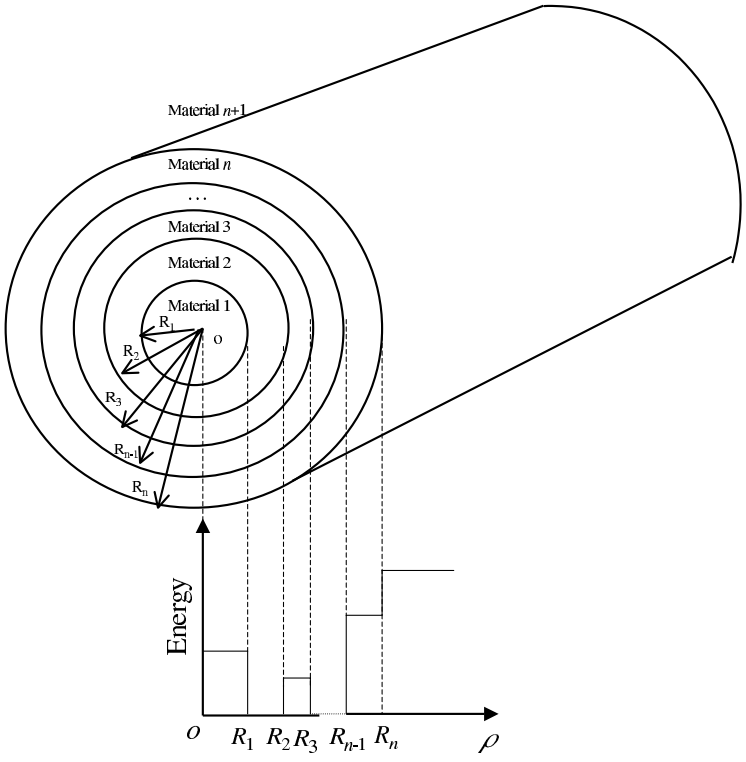

Figure 1. The schematic structure of the multilayer coaxial cylindrical quantum cable system and its potential profile.

2. Theory

Under the dielectric continuum approximation, and starting from the classic electrostatics equations, we have

$$\mathbf{D} = \epsilon\mathbf{E} = \mathbf{E} + 4\pi\mathbf{P}, \tag{1}$$

$$\mathbf{E} = -\nabla\phi(\mathbf{r}), \tag{2}$$

$$\nabla \cdot \mathbf{D} = 4\pi\rho_0(\mathbf{r}). \tag{3}$$

For free oscillation, the charge density $\rho_0(\mathbf{r}) = 0$, so we get the equation

$$\epsilon\nabla^2\phi(\mathbf{r}) = 0 \tag{4}$$

with

$$\epsilon(\omega) = \epsilon_\infty + \frac{\epsilon_0 - \epsilon_\infty}{1 - \omega^2/\omega_{TO}^2}, \tag{5}$$

where ϵ_0, ϵ_∞ are the static and high-frequency dielectric constants and ω_{TO} is the frequency of transverse-optical phonon.

There are two possible solutions to equation(4); one is

$$\epsilon(\omega) = 0, \tag{6}$$

and the other being

$$\nabla^2\phi(\mathbf{r}) = 0. \tag{7}$$

2.1. Confined LO phonon modes

To the first solution, via equation (5) and the Lyddane-Sachs-Teller (LST) relation, one can get

$$\omega^2 = \omega_{\mathrm{TO}}^2\frac{\epsilon_0}{\epsilon_\infty} = \omega_{\mathrm{LO}}^2, \tag{8}$$

which describes the confined bulk LO modes of frequency $\omega = \omega_{\mathrm{LO}}$, where ω_{LO} is the frequency of the LO phonon.

For the LO phonon modes in the core region ($R_0 \le \rho \le R_1$, and $R_0 = 0$) and in each shell region ($R_{i-1} \le \rho \le R_i$, $i = 2, 3, \ldots, n+1$, and $R_{n+1} \to \infty$), because $\epsilon(\omega_{\mathrm{LO}i}) \equiv 0$, the eigenfunctions [17, 21–22] in equation (7) can be arbitrary functions of $\mathbf{r}$, which need only satisfy the boundary condition that the eigenfunctions should be zero at $\rho = R_{i-1}$, R_i. Thus, the eigenfunctions for the LO phonon modes can be chosen as

$$\phi_{lmk_z}^{\mathrm{LO}i}(\mathbf{r}) = \begin{cases} A_{lm}^{\mathrm{LO1}} J_l(\frac{\chi_{lm}}{R_1}\rho)\mathrm{e}^{\mathrm{i}m\varphi}\mathrm{e}^{\mathrm{i}k_z z} & R_0 \le \rho \le R_1 (i=1) \\ A_{lm}^{\mathrm{LO}i} T_{lm}^{\mathrm{LO}i}(\frac{a_{lm}}{R_{i-1}}\rho)\mathrm{e}^{\mathrm{i}m\varphi}\mathrm{e}^{\mathrm{i}k_z z} & R_{i-1} \le \rho \le R_i (i=2,3,\ldots,n+1) \end{cases}, \tag{9}$$

where $T_{lm}^{\mathrm{LO}i}(a_{lm}/R_{i-1}\rho)$ is a radial function we constructed for LOi ($i = 2, 3, \ldots, n+1$) phonon modes, and is given by

$$T_{lm}^{\mathrm{LO}i}\left(\frac{a_{lm}}{R_{i-1}}\rho\right) = J_l\left(\frac{a_{lm}}{R_{i-1}}\rho\right) + b_{lm}Y_l\left(\frac{a_{lm}}{R_{i-1}}\rho\right), \tag{10}$$

where $J_l(x)$ and $Y_l(x)$ are the Bessel function and the Bessel function of the second kind of order l, respectively. χ_{lm} is the m^{th} zero of $J_l(x)$, namely, $J_l(\chi_{lm}) \equiv 0$. The function constructed $T_{lm}^{\text{LO}i}(a_{lm}\rho/R_{i-1})$ satisfies the boundary conditions at $\rho = R_{i-1}$ and $\rho = R_i$. That is,

$$\begin{aligned} T_{lm}^{\text{LO}i}(\frac{a_{lm}}{R_{i-1}}\rho)|_{\rho=R_{i-1}} &= J_l(a_{lm}) + b_{lm}Y_l(a_{lm}) = 0, \\ T_{lm}^{\text{LO}i}(\frac{a_{lm}}{R_{i-1}}\rho)|_{\rho=R_i} &= J_l(\frac{a_{lm}}{R_{i-1}}R_i) + b_{lm}Y_l(\frac{a_{lm}}{R_{i-1}}R_i) = 0, \end{aligned} \tag{11}$$

so a_{lm} and b_{lm} can be solved by equations (11). m in the radial function $T_{lm}^{\text{LO}i}(a_{lm}\rho/R_{i-1})$ denotes the number of zeros within the range of $R_{i-1} \le \rho \le R_i$ $(i = 2, 3, \ldots, n+1)$. Thus, the polarization fields for the LO phonon modes of the system are obtained by $\mathbf{P} = 1/4\pi\nabla\phi$, namely,

$$\begin{aligned} \mathbf{P}_{lmk_z}^{\text{LO1}} &= \frac{1}{4\pi}\nabla\phi_{lmk_z}^{\text{LO1}} \\ &= \frac{A_{lm}^{\text{LO1}}}{4\pi}\left\{\frac{1}{2}\left[J_{l-1}\left(\frac{\chi_{lm}}{R_1}\rho\right) - J_{l+1}\left(\frac{\chi_{lm}}{R_1}\rho\right)\right]\frac{\chi_{lm}}{R_1}\mathbf{e}_\rho \right. \\ &\quad \left. + J_l\left(\frac{\chi_{lm}}{R_1}\rho\right)\frac{\mathtt{i}m}{\rho}\mathbf{e}_\varphi + J_l\left(\frac{\chi_{lm}}{R_1}\rho\right)\mathtt{i}k_z\mathbf{e}_z\right\}\mathtt{e}^{\mathtt{i}m\varphi}\mathtt{e}^{\mathtt{i}k_z z}, \end{aligned} \tag{12}$$

and

$$\begin{aligned} \mathbf{P}_{lmk_z}^{\text{LO}i} &= \tfrac{1}{4\pi}\nabla\phi_{lmk_z}^{\text{LO}i} \\ &= \tfrac{A_{lm}^{\text{LO}i}}{4\pi}\left\{\tfrac{1}{2}\left[T_{l-1,m}(\tfrac{a_{lm}}{R_{i-1}}\rho)\right.\right. \\ &\quad \left.-T_{l+1,m}(\tfrac{a_{lm}}{R_{i-1}}\rho)\right]\tfrac{a_{lm}}{R_{i-1}}\mathbf{e}_\rho \qquad ,(i = 2, 3, \ldots, n+1) \\ &\quad +T_{lm}(\tfrac{a_{lm}}{R_{i-1}}\rho)\tfrac{\mathtt{i}m}{\rho}\mathbf{e}_\varphi \\ &\quad \left.+T_{lm}(\tfrac{a_{lm}}{R_{i-1}}\rho)\mathtt{i}k_z\mathbf{e}_z\right\}\mathtt{e}^{\mathtt{i}m\varphi}\mathtt{e}^{\mathtt{i}k_z z}. \end{aligned} \tag{13}$$

It is easy to get the orthogonal relation for the polarization vector of the LO phonons $\mathbf{P}_{lmk_z}^{\text{LO}i}$, i.e.,

$$\begin{aligned} &\int \mathbf{P}_{l'm'k'_z}^{\text{LO1}^*} \cdot \mathbf{P}_{lmk_z}^{\text{LO1}}\mathtt{d}^3\mathbf{r} \\ &= \frac{L\left|A_{lm}^{\text{LO1}}\right|^2}{8\pi}\left\{\frac{1}{2}(\chi_{lm}^2 + R_1^2k_z^2)J_{l+1}^2(\chi_{lm})\right\}\delta_{l'l}\delta_{m'm}\delta_{k'_z k_z}, \end{aligned} \tag{14}$$

$$\begin{aligned} &\int \mathbf{P}_{l'm'k'_z}^{LOi^*} \cdot \mathbf{P}_{lmk_z}^{\text{LO}i}\mathtt{d}^3\mathbf{r} \\ &= \tfrac{L\left|A_{lm}^{\text{LO}i}\right|^2}{32\pi}\{a_{lm}^2[\gamma^2T_{l-1,m}^2(a_{lm}\gamma) + \gamma^2T_{l+1,m}^2(a_{lm}\gamma) - T_{l-1,m}^2(a_{lm}) \quad (\mathtt{i} = \mathtt{2}, \mathtt{3}, \ldots, \mathtt{n}+\mathtt{1}) \\ &-T_{l+1,m}^2(a_{lm})] - 2k_z^2R_{i-1}^2[\gamma^2T_{l-1,m}(a_{lm}\gamma)T_{l+1,m}(a_{lm}\gamma) \\ &-T_{l-1,m}(a_{lm})T_{l+1,m}(a_{lm})]\}\delta_{l'l}\delta_{m'm}\delta_{k'_z k_z}, \end{aligned} \tag{15}$$

where L is the length of the QC, and γ_i is defined as R_i/R_{i-1}.

In order to derive the free-phonon Hamiltonian, we need the dynamic equation of motion of the crystal lattice [38]:

$$\mu\ddot{\mathbf{u}} = \mu\omega_0^2\mathbf{u} + e\mathbf{E}_{loc}, \tag{16}$$

$$\mathbf{P} = n^*e\mathbf{u} + n^*\alpha\mathbf{E}_{loc}, \tag{17}$$

where μ is the reduced mass of the ion pair and $\mathbf{u} = \mathbf{u}_+ - \mathbf{u}_-$ is the relative displacement of the positive and negative ions, ω_0 is the frequency associated with the short-range force between ions, n^* is the number

of ion pairs per unit volume, and α is the electronic polarizability per ion pair, and $\mathbf{E}_{loc}$ is the local field at the position of the ions. The Hamiltonian of the free vibration is given by

$$H_{\mathtt{ph}} = \frac{1}{2}\int [n^*\mu\ \dot{\mathbf{u}}\cdot\dot{\mathbf{u}} + n^*\mu\omega_0^2\mathbf{u}\cdot\mathbf{u} - n^* e\mathbf{u}\cdot\mathbf{E}_{loc}]\mathtt{d}^3\mathbf{r}. \tag{18}$$

For LO phonon modes, making use of the well-known Lorentz relation $\mathbf{E}_{loc} = \mathbf{E} + 4\pi\mathbf{P}/3$, the relation $\mathbf{E} = -4\pi\mathbf{P}$ (noting $\epsilon(\omega) = 0$) and equation (18), we have

$$\mathbf{E}_{loc} = -\frac{8}{3}\pi\mathbf{P}, \tag{19}$$

$$\mathbf{u} = \frac{1+\frac{8}{3}\pi n^*\alpha}{n^* e}\mathbf{P}. \tag{20}$$

Substituting equation (20) into equation (18), we can write the confined LO phonon Hamiltonian as

$$H_{LO} = \frac{1}{2}\int [n^*\mu(\frac{1+\frac{8}{3}\pi n^*\alpha}{n^* e})^2\ \dot{\mathbf{P}^*}\cdot\dot{\mathbf{P}} + n^*\mu\omega_{\mathrm{LO1}}^2(\frac{1+\frac{8}{3}\pi n^*\alpha}{n^* e})^2\mathbf{P}^*\cdot\mathbf{P}]\mathtt{d}^3\mathbf{r}, \tag{21}$$

Substituting relations (14) or (16) into equation (21), it can be see that, if we choose $A_{lm}^{\mathrm{LO}i}$ to be

$$\left|A_{lm}^{\mathrm{LO}i}\right|^2 = \frac{16\pi}{n^*\mu L}\left(\frac{n^* e}{1+8\pi n^*\alpha/3}\right)^2 \times \tag{22}$$
$$\begin{cases} \left[(\chi_{lm}^2 + R_1^2 k_z^2)J_{l+1}^2(\chi_{lm})\right]^{-1}, & i = 1 \\ 2\{a_{lm}^2[\gamma_i^2 T_{l-1,m}^2(a_{lm}\gamma_i) + \gamma_i^2 T_{l+1,m}^2(a_{lm}\gamma_i) - T_{l-1,m}^2(a_{lm}) \\ \quad -T_{l+1,m}^2(a_{lm})] - 2k_z^2 R_{i-1}^2[\gamma_i^2 T_{l-1,m}(a_{lm}\gamma_i)T_{l+1,m}(a_{lm}\gamma_i) & i = 2,3,\ldots n+1 \\ \quad -T_{l-1,m}(a_{lm})T_{l+1,m}(a_{lm})]\}^{-1} \end{cases},$$

then $\mathbf{P}_{lmk_z}^{\mathrm{LO}i}$ may form an orthonormal and complete set. We introduce creation and annihilation operators $a_{lmn}^\dagger$ and a_{lmn} to express the polarization vector $\mathbf{P}^{\mathrm{LO}i}$ and the standard Hamiltonian $H_{\mathrm{LO}i}$:

$$\mathbf{P}^{\mathrm{LO}i} = \sum_{lmk_z}(\frac{\hbar}{\omega_{\mathrm{LO}i}})^{\frac{1}{2}}[a_{lm}^\dagger(k_z) + a_{lm}(k_z)]\mathbf{P}_{lmk_z}^{\mathrm{LO}i}, \tag{23}$$

$$\dot{\mathbf{P}}^{\mathrm{LO}i} = -\mathtt{i}\sum_{lmk_z}(\hbar\omega_{\mathrm{LO}i})^{\frac{1}{2}}[a_{lm}^\dagger(k_z) - a_{lm}(k_z)]\mathbf{P}_{lmk_z}^{\mathrm{LO}i}, \tag{24}$$

$$H_{\mathrm{LO}i} = \sum_{lmk_z}\hbar\omega_{\mathrm{LO}i}[a_{lm}^\dagger(k_z)a_{lm}(k_z) + \frac{1}{2}]. \tag{25}$$

The operators for the LOi phonon of the lmk_z satisfy commutation relation

$$[a_{lm}(k_z), a_{l'm'}^\dagger(k_z')] = \delta_{l'l}\delta_{m'm}\delta(k_z' - k_z), \tag{26}$$

$$[a_{lm}(k_z), a_{l'm'}(k_z')] = [a_{lm}^\dagger(k_z), a_{l'm'}^\dagger(k_z')] = 0. \tag{27}$$

The eigenfunction of the LOi phonon modes $\phi(\mathbf{r})$ could be expanded in term of the normal modes, so the Fröhlich Hamiltonian between the electron and LOi phonon is derived as

$$H_{e-\mathrm{LO}i} = -e\phi^{\mathrm{LO}i}(\mathbf{r}) \tag{28}$$
$$= -\sum_{lmk_z}\left[\Gamma_{lm}^{\mathrm{LO}i}\mathtt{e}^{\mathtt{i}m\varphi}\mathtt{e}^{\mathtt{i}k_z z}a_{lm}^\dagger(k_z)\times\begin{cases} J_l(\frac{\chi_{lm}}{R_1}\rho) & i = 1 \\ T_{lm}^{\mathrm{LO}i}(\frac{a_{lm}}{R_{i-1}}\rho) & i = 2,3,\ldots,n+1 \end{cases} + \mathtt{H.c.}\right],$$

where

$$\begin{aligned}
&\left|\Gamma_{lm}^{\mathrm{LO}i}\right|^2 \\
= &\left|A_{lm}^{\mathrm{LO}i}\right|^2 \frac{e^2\hbar}{\omega_{\mathrm{LO}i}} \\
= &\frac{4e^2\hbar\omega_{\mathrm{LO}i}}{L}(\frac{1}{\epsilon_{i\infty}}-\frac{1}{\epsilon_{i0}})\times \\
&\begin{cases} [(\chi_{lm}^2+R_1^2k_z^2)J_{l+1}^2(\chi_{lm})]^{-1}, & i=1 \\ 2\times\{a_{lm}^2[\gamma_i^2T_{l-1,m}^2(a_{lm}\gamma)+\gamma_i^2T_{l+1,m}^2(a_{lm}\gamma)-T_{l-1,m}^2(a_{lm}) \\ -T_{l+1,m}^2(a_{lm})]-2k_z^2R_{i-1}^2[\gamma_i^2T_{l-1,m}(a_{lm}\gamma_i)T_{l+1,m}(a_{lm}\gamma_i) & i=2,3,...,n+1 \\ -T_{l-1,m}(a_{lm})T_{l+1,m}(a_{lm})]\}^{-1} \end{cases}.
\end{aligned} \tag{29}$$

2.2. The IO phonon modes

The second possible solution of electrostatic equation (4) is Laplace equation (7), and it will give the IO phonon modes. For IO phonon modes, because $\epsilon(\omega)\neq 0$, via equation (17), (18), we have [37]

$$\mathbf{E}_{loc}=\frac{\mu}{e}(\omega_0^2-\omega^2)\mathbf{u}, \tag{30}$$

$$\mathbf{u}=\frac{\mathbf{P}}{n^*e[1+(\alpha\mu/e^2)(\omega_0^2-\omega^2)]}. \tag{31}$$

Following equation (21), we then get the Hamiltonian for the IO phonon as

$$\begin{aligned}
H_{\mathrm{IO}} = &\frac{1}{2}\int[n^*\mu(\frac{1}{n^*e[1+(\alpha\mu/e^2)(\omega_0^2-\omega^2)]})^2\,\dot{\mathbf{P}}^*\cdot\dot{\mathbf{P}} \\
&+n^*\mu\omega^2(\frac{1}{n^*e[1+(\alpha\mu/e^2)(\omega_0^2-\omega^2)]})^2\mathbf{P}^*\cdot\mathbf{P}]\mathtt{d}^3\mathbf{r}.
\end{aligned} \tag{32}$$

Taking the phonon potentials couplings between the IO phonons into account, the IO phonon electrostatic potential in an n-layer coaxial cylindrical QC system can be written as

$$\phi(\mathbf{r})=\sum_{m,k_z}\sum_{i=1}^{n+1}\{\mathtt{e}^{\mathtt{i}m\varphi}\mathtt{e}^{\mathtt{i}k_zz}[A_iI_m(k_z\rho)+B_iK_m(k_z\rho)]\theta(R_i-\rho)\theta(\rho-R_{i-1})\}, \tag{33}$$

where $K_m(x)$ and $I_m(x)$ are the first and second kind modified Bessel functions, respectively, and $\theta(\rho)$ is the step function. In order to guarantee the potential functions of phonon being limited at $\rho=0$ and ∞, the conditions of $A_{n+1}=B_1=0$ should be satisfied. The continuity of the phonon potential functions and their normal components of electric displace at $\rho=R_i$ $(i=1,2,\ldots,n)$ imply

$$\begin{cases} \phi_i^{m,k_z}(\mathbf{r})|_{\rho=R_i}=\phi_{i+1}^{m,k_z}(\mathbf{r})|_{\rho=R_i} \\ \epsilon_i(\omega)\frac{\partial\phi_i^{m,k_z}(\mathbf{r})}{\partial\rho}|_{\rho=R_i}=\epsilon_{i+1}(\omega)\frac{\partial\phi_{i+1}^{m,k_z}(\mathbf{r})}{\partial\rho}|_{\rho=R_i} \end{cases},i=1,2,\ldots,\mathtt{n}. \tag{34}$$

Other than the LO phonons, the dielectric functions $\epsilon_i(\omega)$ of the IO phonons are not zero and they are given by Eq. (5) and the LST relations as

$$\epsilon_i(\omega)=\epsilon_{i\infty}\frac{\omega^2-\omega_{\mathrm{LO}i}^2}{\omega^2-\omega_{TOi}^2},i=1,2,\ldots,\mathtt{n}+1, \tag{35}$$

where $\epsilon_{i\infty}$ is high-frequency dielectric constant of ith layer material, and $\omega_{\mathrm{LO}i}$ and ω_{TOi} are the corresponding frequencies of longitudinal-optical and transverse-optical vibrations. We define the 2×2 matrices

$$\mathbf{M}_i=\begin{pmatrix} I_m(k_zR_i) & K_m(k_zR_i) \\ \epsilon_iI_m'(k_z\rho)|_{\rho=R_i} & \epsilon_iK_m'(k_z\rho)|_{\rho=R_i} \end{pmatrix}, \tag{36}$$

$$\mathbf{M}'_i = \begin{pmatrix} I_m(k_z R_i) & K_m(k_z R_i) \\ \epsilon_{i+1} I'_m(k_z\rho)|_{\rho=R_i} & \epsilon_{i+1} K'_m(k_z\rho)|_{\rho=R_i} \end{pmatrix}, \tag{37}$$

and the vectors

$$\mathbf{C}_i = \begin{pmatrix} A_i \\ B_i \end{pmatrix}, \tag{38}$$

then Eqs (34) can be expressed by

$$\mathbf{M}_i \mathbf{C}_i = \mathbf{M}'_i \mathbf{C}_{i+1}, (i = 1, 2, \ldots, \mathtt{n}). \tag{39}$$

Via solving the inverse matrix, it is easy to derive the relation

$$\mathbf{C}_i = (\prod_{j=i}^{n-1} \mathbf{D}_j)\mathbf{C}_n, \tag{40}$$

where

$$\mathbf{D}_i = \mathbf{M}_i^{-1} \cdot \mathbf{M}'_i. \tag{41}$$

It should be noted that, when the factorial for matrix $\mathbf{D}_j$ in Eq. (40) is calculated, the order of calculation of matrix should be done from right to left. In particular, when $i = 1$, via Eq.(40), one can get

$$\mathbf{C}_1 = \prod_{j=1}^{n-1} \mathbf{D}_j \mathbf{C}_n. \tag{42}$$

Moreover, we notice that $A_{n+1} = B_1 = 0$ in Eq (33). Via this condition and Eq. (42), the next relation is obtained:

$$B_1 = \left[\prod_{j=1}^{n-1} \mathbf{D}_j\right]_{2,2} = 0, \tag{43}$$

which just gives the dispersion relation for the IO phonon modes. Substituting dielectric functions Eqs (35) into above Eq. (43), the dispersion frequencies ω for the IO phonons are solved. When ω is worked out, the values for dielectric functions can be obtained by Eq.(35). Thus, the rest coefficients in the electrostatic potential function can be expressed by B_{n+1}, and they are given by

$$A_i = \left[\prod_{j=i}^{n-1} \mathbf{D}_j\right]_{1,2} B_{n+1} = g_i B_{n+1}, \tag{44}$$

$$B_i = \left[\prod_{j=i}^{n-1} \mathbf{D}_j\right]_{2,2} B_{n+1} = h_i B_{n+1}. \tag{45}$$

Using eqs. (44) and (45), the phonon potential function (33) can be rewritten as

$$\phi(\mathbf{r}) = B_{n+1} \sum_{m,k_z} \sum_{i=1}^{n+1} \{\mathtt{e}^{\mathtt{i}m\varphi} \mathtt{e}^{\mathtt{i}k_z z} [g_i I_m(k_z\rho) + h_i K_m(k_z\rho)]\theta(R_i - \rho)\theta(\rho - R_{i-1})\}. \tag{46}$$

Thus, the polarization fields for the IO phonon modes of the system are obtained by $\mathbf{P}=(1-\epsilon)/4\pi\nabla\phi$,

$$\begin{aligned}\mathbf{P}^{\mathtt{IO}}_{m,k_z} &= \frac{1-\epsilon}{4\pi}\nabla\phi(\mathbf{r})_{m,k_z} \\ &= \frac{B_{n+1}}{4\pi}\sum_{i=1}^{n+1}(1-\epsilon_i)\nabla\{\mathtt{e}^{\mathtt{i}m\varphi}\mathtt{e}^{\mathtt{i}k_z z}[g_i I_m(k_z\rho)+h_i K_m(k_z\rho)]\theta(R_i-\rho)\theta(\rho-R_{i-1})\}.\end{aligned} \tag{47}$$

It is easy to get the orthogonal relation for the polarization vector of IO phonon $\mathbf{P}^{\mathtt{IO}}_{m,k_z}$,

$$\begin{aligned}&\int \mathbf{P}^{\mathtt{IO}^*}_{m'k'_z}\cdot\mathbf{P}^{\mathtt{IO}}_{mk_z}\mathtt{d}^3\mathbf{r} \\ =\ & \frac{|B_{n+1}|^2 k_z^2 L}{16\pi}\{\sum_{i=1}^{n+1}(1-\epsilon_i)^2\int_{R_{i-1}}^{R_i}\{[g_i^2(I_{m-1}^2+I_{m+1}^2+2I_m^2)+h_i^2(K_{m-1}^2+K_{m+1}^2+2K_m^2)] \\ &+2g_ih_i(2I_mK_m-I_{m-1}K_{m-1}-I_{m+1}K_{m+1})\}\rho\mathtt{d}\rho\}\delta_{m'm}\delta_{k'_zk_z}.\end{aligned} \tag{48}$$

Using the orthogonal relation of the polarization vector (48) and choosing

$$|B_{n+1}|^{-2}=\frac{k_z^2L}{2\omega^2}\{\sum_{i=1}^{n+1}(\frac{1}{\epsilon_i-\epsilon_{i0}}-\frac{1}{\epsilon_i-\epsilon_{i\infty}})^{-1}\mathtt{Int}(i,m,k_z)\} \tag{49}$$

with

$$\begin{aligned}\mathtt{Int}(i,m,k_z) &= \int_{R_{i-1}}^{R_i}\rho\mathtt{d}\rho\{[g_i^2(I_{m-1}^2+I_{m+1}^2+2I_m^2)+h_i^2(K_{m-1}^2+K_{m+1}^2+2K_m^2)] \\ &\quad +2g_ih_i(2I_mK_m-I_{m-1}K_{m-1}-I_{m+1}K_{m+1})\},\end{aligned} \tag{50}$$

we can make $\mathbf{P}^{\mathtt{IO}}_{m,k_z}$ form orthonormal and complete sets, which can be used to express the IO phonon field $H_{\mathtt{IO}}$ and the electron-phonon interaction Hamiltonian $H_{e-\mathtt{IO}}$. Then the IO phonon field is given as

$$H_{\mathtt{IO}}=\sum_{mk_z}\hbar\omega\left[b_m^\dagger(k_z)b_m(k_z)+\frac{1}{2}\right], \tag{51}$$

where $b_m^\dagger(k_z)$ and $b_m(k_z)$ were creation and annihilation operator for IO phonon of the (m,k_z)th mode. They satisfied the commutative rules for bosons.

$$\begin{aligned}[b_m(k_z),b_{m'}^\dagger(k'_z)] &= \delta_{m'm}\delta_{k'_zk_z}, \\ [b_m(k_z),b_{m'}(k'_z)] &= [b_m^\dagger(k_z),b_{m'}^\dagger(k'_z)]=0.\end{aligned} \tag{52}$$

The Fröhlich Hamiltonian describing the interaction between the electron and the IO phonon is given by

$$H_{e-\mathtt{IO}}=-\sum_{mk_z}\Gamma^{\mathtt{IO}}_{m,k_zR_1}(\rho)[b_m(k_z)\mathtt{e}^{\mathtt{i}m\varphi}\mathtt{e}^{\mathtt{i}k_zz}+\mathtt{H.c.}], \tag{53}$$

where $\Gamma^{\mathtt{IO}}_{m,k_zR_1}(\rho)$ was the coupling function which was defined as

$$\begin{aligned}\Gamma^{\mathtt{IO}}_{m,k_zR_1}(\rho) &= N_{m,k_z}\times f_m(k_z\rho) \\ &= N_{m,k_z}\sum_{i=1}^{n+1}[g_iI_m(k_z\rho)+h_iK_m(k_z\rho)]\theta(R_i-\rho)\theta(\rho-R_{i-1})\end{aligned} \tag{54}$$

with

$$|N_{m,k_z}|^2=\frac{2\hbar\omega e^2}{k_z^2L}\{\sum_{i=1}^{n+1}(\frac{1}{\epsilon_i-\epsilon_{i0}}-\frac{1}{\epsilon_i-\epsilon_{i\infty}})^{-1}\mathtt{Int}(i,m,k_z)\}^{-1}. \tag{55}$$

3. Numerical Results and Discussion

In order to see more clearly the behaviors of the phonon modes in the multi-layer coaxial cylindrical QCs, as an example, numerical calculations on a four-layer QC system made by GaAs/$Ga_{1-x}Al_xAs$ materials have been performed. Due to the simplicity of the electron-LO phonon coupling functions, which are just the oscillating and attenuating Bessel functions, thus, the next discussions mainly focus on the dispersion frequencies for the IO phonons and their couplings with electrons. The material parameters originate from Ref. [39] and are listed in Table 1.

Table 1. The material parameters [39].

	Material parameters		
	GaAs	$Ga_{1-x}Al_xAs$	AlAs
$\hbar\omega_{LO}$ (meV)	36.25	$36.25 + 3.83x + 17.12x^2 - 5.11x^3$	50.09
$\hbar\omega_{TO}$ (meV)	33.29	$33.29 + 10.70x + 0.03x^2 + 0.86x^3$	44.88
ε_0	13.18	$13.18 - 3.12x$	10.06
ε_∞	10.89	$10.89 - 2.73x$	8.16

Figure 2 shows the dispersion frequencies of the IO modes $\hbar\omega$ as functions of the phonon wave-vector in the z direction k_z in the four-layer $Ga_{0.8}Al_{0.2}As$/GaAs- /$Ga_{0.9}Al_{0.1}As$/$Ga_{0.6}Al_{0.4}As$ QC system with thicknesses 5 nm/5 nm/5 nm/∞. (In the following figures, the structure of the QC is kept unchanged.) In fact, the azimuthal quantum number m is kept at 0. Other than the inhomogeneous QDQW system [37], in which the dispersion frequencies are a discrete function of the quantum number since there is no wave vector in the QC system, the dispersion frequencies can be a continuum function of the wave vector in the z direction. From the figure, it is observed that there are six branches of IO phonon modes, labeled 1, 2, 3, 4, 5 and 6 in order of the increasing frequency (i.e. Eq. (43) has just six solutions for ω). When k_z is small (such as $k_zR_1 \leq 1$), the dispersions are more obvious; but when k_z is relatively big (such as $k_zR_1 \geq 1.5$), the dispersions for each mode almost can be negligible. In detailed calculations for $k_z \to 0$, the frequencies of the six branches the IO phonon modes (mode 1 to mode 6) are found to approach $\omega_{\mathrm{TO}2}$, $\omega_{\mathrm{TO}3}$, $\omega_{\mathrm{TO}1}$, $\omega_{\mathrm{LO}2}$, $\omega_{\mathrm{LO}3}$ and $\omega_{\mathrm{LO}4}$, respectively. It is noted that, $\omega_{\mathrm{TO}1}$ and $\omega_{\mathrm{LO}4}$ appear, but $\omega_{\mathrm{LO}1}$ and ω_{TO4} are forbidden. The frequencies forbidden behaviors in the QC are obviously different from the case in a multi-layer asymmetrical planer hetero system [16, 18]. In the asymmetrical planer hetero system, when the wave-vector in z direction $k_z \to 0$, both frequencies of the TO and LO phonons in the outermost-layer materials were forbidden, but two new frequencies ω_+ and ω_- appeared. This difference of the IO phonon limit ($k_z \to 0$) frequencies in the two systems may originate from the distinctions of the symmetry of the two quantum systems, namely, one is a planar symmetrical system, and the other is an axial symmetrical system. On the other hand, when $k_z \to \infty$, the frequency of each branch of the IO phonon approaches a constant. In order to distinguish and label the six branches of the IO phonon modes, the limit frequencies of the IO phonons when $k_z \to \infty$ in the homogeneous cylindrical QWW formed by the two materials on both sides of the three interfaces are listed in Table 2. These limit frequency values can be computed by the equation $\epsilon_1(\omega)/\epsilon_2(\omega) = -K_m(k_zR_1)I'_m(k_zr)|_{r=R_1}/[I_m(k_zR_1)K'_m(k_zr)|_{r=R_1}]$ [33], which determines the IO phonon frequencies in a single heterostructure. It is well known that, when $x \to \infty$, $I_m(x)$ and $K_m(x)$ approach $e^x/\sqrt{2\pi x}$ and $e^{-x}\sqrt{\pi}/\sqrt{2x}$, respectively, so $\epsilon_1(\omega)/\epsilon_2(\omega) \to -1$. Via this relation, it is easy to calculate the two limit frequency values of the IO phonon in the single heterostructure. The branch with lower frequency is labeled by $\hbar\omega_{iL}$; the other branch, with higher frequency, is labeled by $\hbar\omega_{iH}$; and the index i in Table 2 denotes the i th interface. According to the data in Table 2, it is easy to label the six IO phonon modes in Figure 2. For example, $2H$ and $2L$ denote the two modes mainly localized in the vicinity of the second interface (these characters can be seen clearly in Figure 4), and they represent the higher frequency branch and lower frequency branch at the second interface, respectively.

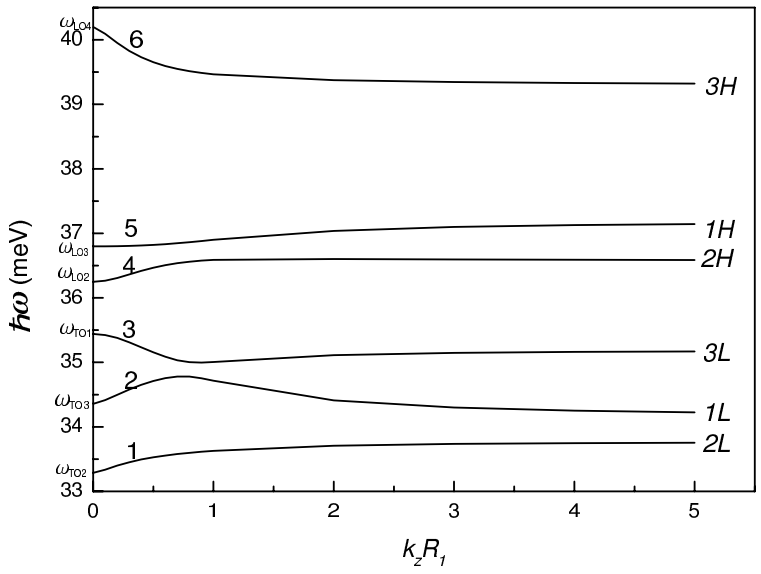

Figure 2. The dispersion frequencies $\hbar\omega$ as functions of k_z in a four-layer $Ga_{0.8}Al_{0.2}As/GaAs/Ga_{0.9}Al_{0.1}As/Ga_{0.6}Al_{0.4}As$ QC system with thicknesses 5 nm/5 nm/5 nm/∞, with azimuthal quantum number m is kept at 0.

Table 2. The limit frequencies of the IO phonon modes in single heterostructures.

IO phonon limited frequencies in single heterostructures		
Interface materials	$\hbar\omega_{iL}$ (meV)	$\hbar\omega_{iH}$ (meV)
$Al_{0.2}Ga_{0.8}As/GaAs$ $(i = 1)$	34.13	37.20
$GaAs/Al_{0.1}Ga0.9As(i = 2)$	33.78	36.57
$Al_{0.1}Ga_{0.9}As/Al_{0.6}Ga_{0.4}As(i = 3)$	35.20	39.29

In order to investigate the dependence of $\hbar\omega$ on the azimuthal quantum number m, when k_z is kept at $1/2R_1$, phonon frequencies as a function of m are plotted in Figure 3. The frequencies are the discrete functions of quantum number m, and the dash lines in each curve are guided for eyes. Analogous to the case in Figure 2 when m is small, the dispersions are more obvious. As $m \to \infty$, each frequency of the IO phonon also approaches some constant, which is the same as the corresponding limit value in Figure 2. This is not a casual observation. Our calculation reveals that, for a certain x_0, when $m \to \infty$, the value of $K_m(x_0)I'_m(x)|_{x=x_0}/[I_m(x_0)K'_m(x)|_{x=x_0}$ also approaches 1, so the corresponding limit frequencies for large m and k_z converge to the same values. That the observation in Figure 2 and Figure 3 is of physical significance, reveal that only six branches of IO modes with different energies exist in the four-layer QC system. The corresponding polaron may be formed by virtue of the interaction between and electron and these six IO phonon modes [18].

The electron-IO phonon coupling functions $\Gamma^{\mathtt{IO}}_{m,k_zR_1}(\rho)$ as functions of ρ are depicted in Figure 4 for $m = 0$ and 2, and $k_zR_1 = 1$ and 3. Via comparing Figures 4a–4d, it can be seen that, when m and k_z are small (see Figure 4a), the distributions of $\Gamma^{\mathtt{IO}}_{m,k_zR_1}(\rho)$ for each mode on the interfaces are comparatively average, namely, the peaks in the curve at each interface are not very sharp. But with the increasing of k_z or m, the distribution of $\Gamma^{\mathtt{IO}}_{m,k_zR_1}(\rho)$ of each mode tend to be more and more localized at an interface (see Figures 4b–4d), namely, modes 2 and 5 are mainly localized at the first interface $\rho = 5$ nm, modes 1 and 4 are mainly localized at the second interface $\rho = 10$ nm, and modes 3 and 6 are at the third interface $\rho = 15$ nm. So modes 2 and 5 can be seen as the IO modes at the first interface; modes 1 and 4 can be treated as the IO modes at the second interface; and modes 3 and 6 can be treated as IO modes at the third interface. Furthermore, the frequencies of modes 1, 2 and 3 are lower than those of modes 4, 5 and 6. On the basis of

these two features, the six branches of IO phonon modes have been labeled in Figure 2. It is also noticed that, at the position of the origin, $\Gamma_{01}^{\mathrm{IO}}(0)$ and $\Gamma_{03}^{\mathrm{IO}}(0)$ do not equal zero, while $\Gamma_{21}^{\mathrm{IO}}(0)$ and $\Gamma_{23}^{\mathrm{IO}}(0)$ do equal zero, because $I_0(0) \neq 0$ and $I_i(0) = 0$ $(i = 1, 2, \ldots)$.

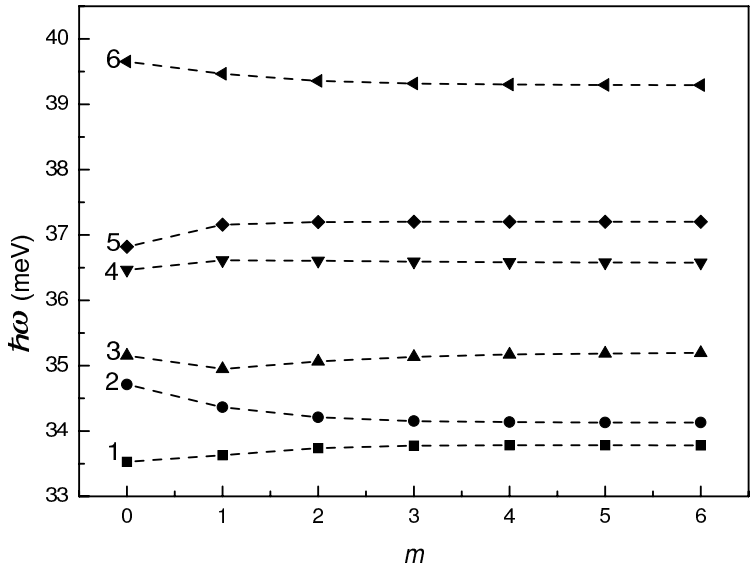

Figure 3. Dispersion frequencies of the IO phonon modes $\hbar\omega$ as a function of m with k_z kept at $1/2R_1$. The signs in the dash lines denote the frequency values, and the dash lines in each curve are guides for the eyes.

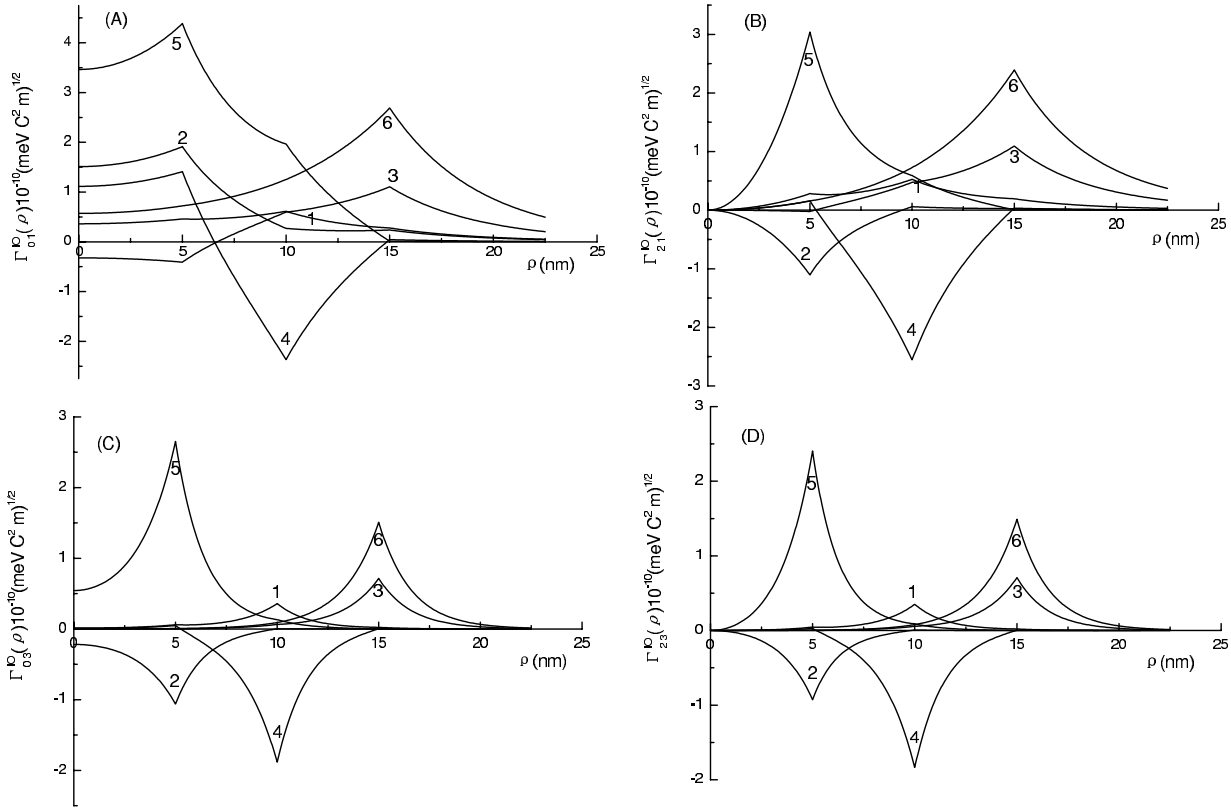

Figure 4. The electron-IO phonon coupling functions $\Gamma_{m,k_z R_1}^{\mathrm{IO}}(\rho)$ as functions of ρ for $m = 0$, 2, and $k_z R_1 = 1$, 3.

In Figure 5, we show the absolute values $\left|\Gamma^{\mathrm{IO}}_{m,k_z R_1}(\rho)\right|$ as a function of k_z for $m = 0$ and 2. According to the analysis in Figure 4, $\rho = 5$ nm is chosen for modes 2 and 5, $\rho = 10$ nm is chosen for modes 1 and 4, and $\rho = 15$ nm for modes 3 and 6. In the case of $m = 0$, when $k_z R_1 < 1.5$, the curves cross each other; but when $k_z R_1 > 2$, each curve decreases monotonically. In the case of $m = 2$ (the embedded figure), as k_z increases from 0, the six curves all decreases monotonically. It is also noticed that, the three branches of phonon modes with higher frequencies 3, 4 and 5 modes, compared with the other three modes with lower frequencies 1, 2 and 3, have stronger coupling with electrons. With this feature specified, the higher frequency IO phonons have more obvious contribution to the electron-phonon interaction in the QC system.

Figure 6 plots the dependence of the absolute values $\left|\Gamma^{\mathrm{IO}}_{m,k_z R_1}(\rho)\right|$ on azimuthal quantum number m when k_z is kept at $1/2R_1$. The same coordinate value in ρ as in Figure 5 for each mode is chosen. With increasing m, modes 1, 2, 5 and 6 decrease monotonically, and modes 3 and 4 have a maximum at $m = 1$. Over the whole range of m, the coupling between the electron and the high frequency phonon modes 4, 5 and 6 is more significant. This character is analogous to the case in the inhomogeneous QDQW system [37].

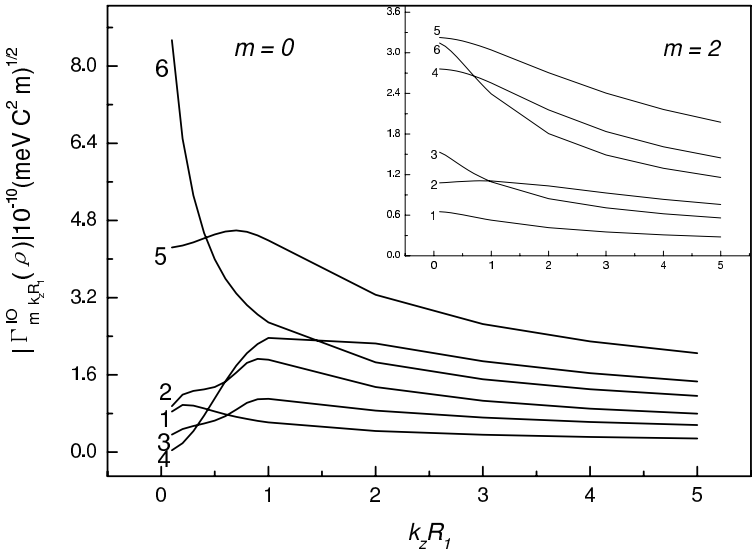

Figure 5. The absolute values $\left|\Gamma^{\mathrm{IO}}_{m,k_z R_1}(\rho)\right|$ as functions of k_z for $m = 0$ and 2.

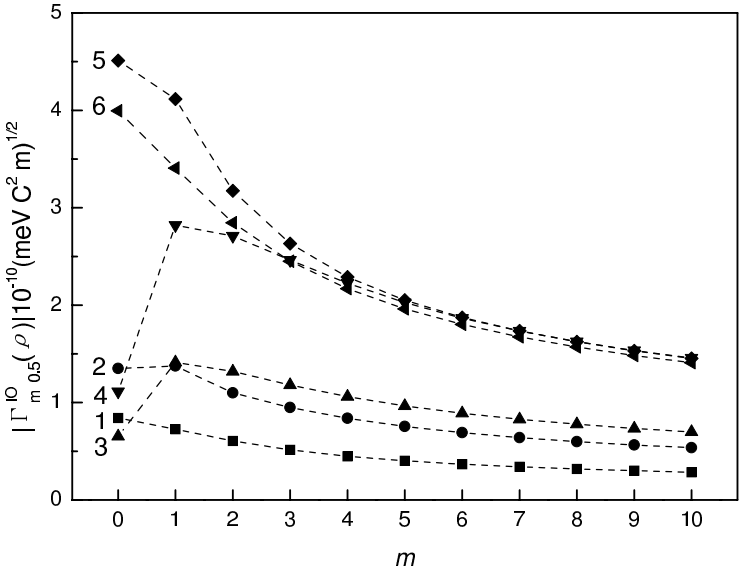

Figure 6. The dependence of the absolute values $\left|\Gamma^{\mathrm{IO}}_{m,k_z R_1}(\rho)\right|$ as functions of m with k_z kept at $1/2R_1$.

Via a comparison of Figure 2 with Figure 3, and Figure 5 with Figure 6, we found the wave-vector in z direction k_z and the azimuthal quantum number m have very analogous effects on the frequencies and the electrostatic potentials of the IO phonons in the QC systems. For example, with increasing m and k_z, the corresponding IO phonon frequencies converge to the same limit frequencies, and the electrostatic potentials tend to be more and more localized at certain interfaces; and the couplings of electron-IO phonon become weaker and weaker. This analogy originates from the fact that, when k_z and m are large enough, the IO modes do not feel the curvature of the wire surfaces [22], so the frequencies and the potential distributions in QCs approach those in plane heterostructure quantum systems.

4. Summary and Conclusions

Under the DC model, the confined LO and IO phonon modes and Fröhlich electron-phonon interaction Hamiltonians in coaxial cylindrical QCs with arbitrary layer-number have been deduced in the present paper. A set of legitimate eigenfunctions for LO phonon modes are constructed to describe the vibration of the LO phonons. Transfer matrix method [19, 20] are employed to deal with the IO phonon modes. Numerical calculations on a four-layer GaAs/Al_xGa_{1-x}As QC have been performed, and the calculations mainly focus on the dispersion relation of IO phonon modes and the coupling function between electron and IO phonon. The main results are as follows:

1. In the inhomogeneous coaxial cylindrical QC model chosen, there exists six branches of IO phonon modes. The curves of the dependences of these dispersion frequencies on the wave-vector in z direction k_z and the azimuthal quantum number m have been plotted. Results reveal that the dispersion is obvious only when k_z and m are small; when k_z and m approach 0, only ω_{LO1} of central region material and ω_{TO4} of the outermost region material are forbidden, which is obviously different from the case in multi-layer planar heterosystem due to the different symmetries of the two models [18]; with increasing k_z and m, the dispersion frequency for each mode converge to a certain IO frequency value in single heterostructure [33], and these observations have reasonable explanation.

2. Study of the coupling function of the electron-IO phonon interaction $\Gamma^{\mathtt{IO}}_{m,k_zR_1}(\rho)$ reveals that, with increasing m and k_z, each phonon mode tends to be more and more localized at interfaces, and the couplings between the electron and the IO phonon become weaker and weaker. Meanwhile, the high frequency phonon modes have more significant contributions to the coupling of the electron-phonon interaction.

3. Via the discussion associated with Figures 2–5, we found the wave-vector in z direction, k_z, and the azimuthal quantum number m have very analogous effects on the frequencies and the electrostatic potentials of the IO phonons. This analogy originates from the observation that the IO modes do not feel the curvature of the wire surfaces for large k_z and m [22], so the frequencies and the potential distributions in QCs approach those in QWs.

From the results of four-layer QC system, it is reasonable to infer, for the n-layer coaxial cylindrical QC system showed as in Figure 1, there exists $2n-2$ ($n \geq 3$) branches of IO phonon modes. It is obvious that the theoretical results described in the present work will contribute the investigation of the IO phonon effects on the physical properties in the QC systems, such as the polaronic effect [40, 41], and the bound polaronic effect [33], the subject of future research projects.

Acknowledgments

The author would like to thank Prof. H. J. Xie for valued discussions. The author is grateful to the referee for reading the first draft.

References

[1] A. Eychmüller, A. Mews, and H. Weller, *Chem. Phys. Lett.*, **208**, (1993), 59.

[2] A. Mews, A. Eychmüller, M. Giersig, D. Schooss, and H. Weller, *J. Phys. Chem.*, **98**, (1994), 934.

[3] A. Eychmüller, T. Vossmeyer, A. Mews and H. Weller, *J. Lumin.*, **58**, (1994), 223.

[4] J. W. Haus, H. S. Zhou, I. Honma and H. Komiyama, *Phys. Rev.*, **B47**, (1993), 1359.

[5] K. Chang and J. B. Xia, *Phys. Rev.*, **B57**, (1998), 9780.

[6] V. Ranjan, and A. S. Vijay, *J. Phys.: Condens. Matt.*, **13**, (2001), 8105.

[7] E. Assaid, E. Feddi, J.E. Khamkhami and F. Dujardin, *J. Phys.: Condens. Matt.*, **15**, (2003), 175.

[8] K. Suenaga, C. Colliex, N. Demoncy, A. Loiseau, H. Pascard and F. Willaime, *Science*, **278**, (1997), 653.

[9] Y. Zhang, K. Suenaga, C. Colliex and S. Iijima, *Science*, **281**, (1998), 973.

[10] Z.Y. Zeng, Y. Xiang and L.D. Zhang, *Eur. Phys. J.*, **B17**, (2000), 699.

[11] S. Aktas, S.E. Okan and H. Akbas, *Superlattic and Microstructure.*, **30**, (2001), 129.

[12] A.K.Sood, J. Menendez, M. Cardona and K. Ploog, *Phys. Rev. Lett.*, **54**, (1985), 2111; **54** 2115; P. Lambin, J.P. Vineron, A.A. Lucas, P.A. Thiry, M. Liehr, J.J. Pireaux, R. Caudano and T.J. Kuech, *ibid.*, **56**, (1986), 1842; M.V. Klein, *IEEE J. Quantum Electron.,* **QE-22**, (1986), 1760.

[13] R. Fuchs and K.L. Kliewer, *Phys. Rev.*, **A140**, (1965), 2076.

[14] J. Licari and R. Evrard, *Phys. Rev.*, **B15**, (1977), 2254.

[15] L. Wendler, *Phys. Stat. Sol. (b)*, **129**, (1985), 513; L. Wendler and R. Haupt, *Phys. Stat. Sol. (b)*, **143**, (1987), 487.

[16] N. Mori and T. Ando, *Phys. Rev.*, **B40**, (1989), 6175.

[17] X.X. Liang and X. Wang, *Phys. Rev.*, **B43**, (1991), 5155.

[18] J. Shi, S. Ling-xi and S. Pan, *Phys. Rev.*, **B47**, (1993), 13 471; J.J. Shi and S. H. Pan, *Phys. Rev.*, **B51**, (1995), 17 681; *J. Appl. Phys.*, **80**, (1996), 3863.

[19] Z.W. Yan and X.X. Liang, *Int. J. Mod. Phys.*, **B15**, (2001), 3539.

[20] S. Yu and K.W. Kim, *J. Appl. Phys.*, **82**, (1997), 3363.

[21] N.C. Constantinou and B.K. Ridley, *Phys. Rev.*, **B41**, (1990), 10, 622; (1990), 10627.

[22] R. Enderlein, *Phys. Rev.*, **B47**, (1993), 2162.

[23] K. Huang and B. Zhu, *Phys. Rev.*, **B38**, (1988), 13 377.

[24] S.F. Ren and Y.C. Chang, *Phys. Rev.*, **B43**, (1991), 11875.

[25] B. Zhu, *Phys. Rev.*, **B44**, (1991), 1926.

[26] F. Rossi, L. Rota, P. Lugli and E. Molinari, *Phys. Rev.*, **B47**, (1993), 1695.

[27] H. Rücker, E. Molinari and P. Lugli, *Phys. Rev.* **B44** (1991) 3463;*Phys. Rev.*, **B45**, (1992), 6747.

[28] M.A. Stroscio, *Phys. Rev.*, **B40**, (1989), 6428; M.A. Stroscio, K.W. Kim, M.A. Littlejohn and H. Chuang, *Phys. Rev.*, **B42**, (1990), 1488.

[29] K.W. Kim, M.A. Strosicio, A. Bhatt, R. Mickevicius and V.V. Mitin, *J. Appl. Phys.*, **70**, (1991), 319.

[30] F. Comas, C. Trallero-Giner and A. Cantarero, *Phys. Rev.*, **B47**, (1993), 7602; F. Comas, A. Cantarero, C. Trallero-Giner and M. Moshinsky, *J. Phys.: Condens Matter*, **7**, (1995), 1789.

[31] J.M. Bergues, R. Betancourt-Riera, R. Riera and J.L. Marin, *J. Phys.: Condens Matter*, **12**, (2000), 7983.

[32] X.F. Wang and X.L. Lei, *Phys. Rev.*, **B49**, (1994), 4780.

[33] H.J. Xie, C.Y. Chen, and B.K. Ma, *Phys. Rev.*, **B61**, (2000) 4827; *J. Phys.: Condens. Matter*, **12**, (2000), 8623.

[34] C.R. Bennett, N.C. Constantinou, M. Babiker and B.K. Ridley, *J. Phys. Condens. Matter*, **7**, (1995), 9819.

[35] P.A. Knipp and T.L. Reinecke, *Phys. Rev.*, **B45**, (1992), 9091; *Phys. Rev.*, **B48**, (1993), 5700.

[36] S.N. Klimin, E.P. Pokatilov and V.M. Fomin, *Phys. stat. sol. (b)*, **184**, (1994), 373.

[37] L. Zhang, H.J. Xie and C.Y. Chen, *Eur. Phys. J.*, **B27**, (2002), 577; *Commun. Theor. Phys.*, **39**, (2003), 238.

[38] M. Born and K. Huang, "*Dynamical Theory of Crystal lattice*", Clarenden Press, Oxford (1954).

[39] S. Adachi, *J. Appl. Phys.*, **58**, (1985), R1.

[40] L. Zhang, H. J. Xie and C. Y. Chen, *Commun. Theor. Phys.* **37** (2002) 755.

[41] C.Y. Chen, W.S. Li, X.Y. Teng and S.D. Liang, Physica, **B245**, (1998), 92.